Atmospheric Environment 84 (2014) 244–253

Contents lists available at ScienceDirect

Atmospheric Environment

journal homepage: www.elsevier.com/locate/atmosenv

Positive relationship between liquid cloud droplet effective radius and aerosol optical depth over Eastern China from satellite data

Jinping Tang [a,b], Pucai Wang [a,*], Loretta J. Mickley [c], Xiangao Xia [a], Hong Liao [d], Xu Yue [c], Li Sun [a,b], Junrong Xia [e]

[a] Key Laboratory of Middle Atmosphere and Global Environment Observation (LAGEO), Institute of Atmospheric Physics, Chinese Academy of Sciences, Beijing 100029, China
[b] University of Chinese Academy Sciences, Beijing 100049, China
[c] School of Engineering and Applied Sciences, Harvard University, Cambridge, MA 02138, USA
[d] State Key Laboratory of Atmospheric Boundary Layer Physics and Atmospheric Chemistry (LAPC), Institute of Atmospheric Physics, Chinese Academy of Sciences, Beijing 100029, China
[e] Key Laboratory for Aerosol-Cloud-Precipitation of China Meteorological Administration, NUIST, Nanjing 210044, China

HIGHLIGHTS

- We studied the first aerosol indirect effect over Eastern China.
- Twomey effect was observed over ocean.
- Positive correlations between aerosol optical depth and cloud effective radius were found over land for most seasons.
- We attributed the positive effect to the associated changes in relative humidity and wind fields.

ARTICLE INFO

Article history:
Received 21 May 2013
Received in revised form
6 August 2013
Accepted 12 August 2013

Keywords:
Aerosol optical depth
Cloud effective radius
Eastern China

ABSTRACT

Correlations between water cloud effective radius (CER) and aerosol optical depth (AOD) from the Moderate Resolution Imaging Spectroradiometer (MODIS) are examined over seven sub-regions in Eastern China for 2003–2012. Water phase cloud is defined as having a cloud top pressure greater than 800 hPa. Significant negative correlation coefficients ($r = -0.79 \sim -0.94$) between AOD and CER are derived over the East Sea and the South China Sea for grid cells with AOD < 0.3. However, positive correlations ($r = 0.01$–0.91) are calculated for cells with AOD > 0.3. In contrast, significant positive correlations ($r = 0.67$–0.95) are derived over the Eastern China mainland and Yellow Sea. Further analysis for North China Plain shows that variations in wind speed and relative humidity may account for such positive correlations. Southerly winds carry high levels of pollutants and abundant water vapor, resulting in coincident increases in both AOD and CER in North China Plain, while the northerly winds transport dry and clean air from high latitudes, leading to decreases in AOD and CER. Both processes contribute to the positive correlations between AOD and CER over Eastern China, suggesting that the influence of background weather conditions need to be considered when studying the interactions between aerosol and cloud.

1. Introduction

By acting as cloud condensation nuclei (CCN), aerosol particles increase cloud droplet number concentration (Ramanathan et al., 2001; Andreae, 2009), limit cloud droplet size at constant liquid water path, and increase cloud albedo; termed the first aerosol indirect effect (FAIE) or Twomey effect (Twomey, 1977; Breon et al., 2002; Feingold et al., 2003). Satellite measurements can provide global observations for statistical studies of the relationships between aerosol and cloud properties. The slopes of correlation analysis evaluated for some parameters have shown some skill in representing the magnitude of FAIE (Nakajima et al., 2001; Feingold et al., 2001; Breon et al., 2002; Sekiguchi et al., 2003; Kaufman et al., 2005; Huang et al., 2006). Uncertainties in the characterization of FAIE include measurement biases and factors such as the size distribution, chemical composition, and mixing state of aerosol

* Corresponding author.
E-mail address: pcwang@mail.iap.ac.cn (P. Wang).

1352-2310/$ – see front matter © 2013 Elsevier Ltd. All rights reserved.
http://dx.doi.org/10.1016/j.atmosenv.2013.08.024

Table 1
Previous studies of the first aerosol indirect effect (FAIE) based on satellite data. IE (unitless) refers to the indirect effect and is the slope of the cloud effective radius (CER) to aerosol index (AI) or to aerosol optical depth (AOD). RF is the estimated radiative forcing due to IE at the top of atmosphere. *Na* is particle number, and *Nc* is cloud droplet number.

Reference	Instrument	Parameter	Region	Result
Nakajima et al., 2001	AVHRR	CER, AI	Global ocean	RF = −0.7 to −1.7 W m^{-2}, IE = 0.17
Feingold et al., 2001	AVHRR	CER, AOD	Amazon	IE = 0.12–0.38
Breon et al., 2002	POLDER	CER, AOD, AI	Global ocean	IE = −0.085 W m^{-2}
Sekiguchi et al., 2003	AVHRR POLDER	CER, *Na*	Global	RF = −0.6 to −1.2 W m^{-2}
Kaufman et al., 2005	MODIS	CER, AOD	Atlantic	△CER = 10%–30%
Yuan et al., 2008	MODIS	CER, AOD	China, Mexico	IE = −2.73–2.03
Costantino and Breon, 2013	MODIS CALIPSO	Vertical profiles	Angola coast	IE = −0.03 to −0.15
Lohmann and Lesins, 2002	POLDER	CER, AI	Global	RF = −0.85 W m^{-2}
Quaas et al., 2006	MODIS POLDER	CER, AOD, AI	Global	RF = −0.3 to −0.5 W m^{-2}
Penner et al., 2012	MODIS CERES	*Nc*, AI TOA fluxes	North Pacific Ocean	RF = −1.8 to −2.2 W m^{-2}

particles, as well as meteorological conditions (Lohmann and Feichter, 2005; Mauger and Norris, 2007). To date, few studies of FAIE using satellite data have been performed over China, where air pollution is heavy and the meteorological environment is complex due to the Asian monsoon (Sekiguchi et al., 2003; Yuan et al., 2008). In this work, FAIE is investigated, and the influence of meteorological conditions is analyzed over seven sub-sectors of Eastern China and the surrounding waters using aerosol and cloud properties observed by the Moderate Resolution Imaging Spectroradiometer (MODIS) and meteorological variables from the European Centre for Medium-Range Weather Forecasts (ECMWF) reanalysis.

An array of approaches has been used to retrieve aerosol and cloud properties from observations. For example, aerosol number concentrations can be measured directly by instruments onboard aircraft (Warner and Twomey, 1967; Andreae et al., 2004) or estimated using aerosol scattering coefficients measured from the ground (Feingold et al., 2003). They may also be represented by column integrated aerosol optical depth (AOD) or aerosol index (AI) measured by satellites (Nakajima et al., 2001; Breon et al., 2002; Kaufman et al., 2005; Huang et al., 2006). Compared with the former two approaches, satellite observations provide a large sample size with high coverage in both space and time, and as a result are more applicable to estimate FAIE on global or regional scales, as outlined in Table 1. In these studies, negative correlations between AOD and cloud effective radius (CER) have been found over oceans (Nakajima et al., 2001; Breon et al., 2002; Kaufman et al., 2005), and positive correlations have been observed over China, the Gulf of Mexico and the Mediterranean Sea (Sekiguchi et al., 2003; Myhre et al., 2007; Yuan et al., 2008). The relationships of aerosol and cloud derived from satellite measurements can be used to constrain climate model simulation and decrease uncertainty of FAIE by a factor of two (Lohmann and Lesins, 2002; Quaas et al., 2006; Penner et al., 2012).

Quantifying FAIE is very uncertain because it is associated with both physical and chemical properties as well as the mixing state of aerosol particles (Nenes et al., 2002; Chen and Penner, 2005; Dusek et al., 2006; Wang et al., 2008), vertical distributions of aerosol and cloud (Costantino and Breon, 2013), and meteorological conditions like relative humidity (RH), wind fields, updraft velocity and lower troposphere static stability (Loeb and Schuster, 2008; Kaufman et al., 2005; Mauger and Norris, 2007; Koren et al., 2010; Wang et al., 2010). For example, large-scale low-level convergence increases cloudiness as well as aerosol number concentration, and relative humidity enhances cloud droplet growth and deliquescence (Mauger and Norris, 2007; Koren et al., 2010). Such effects of meteorology are important, but difficult to isolate from broad observations, like those from satellite.

Pollution in China is characterized by a wide variety of chemical compositions and is influenced by the Asian monsoon, especially in the eastern part of the country (Ding and Chan, 2005; Hu and Ding, 2010; Zhang et al., 2012). Sekiguchi et al. (2003) demonstrated a positive correlation between CER and AI from Polarization and Directionality of the Earth's Reflectances (POLDER) measurements in a 17.5° × 17.5° grid in China. Yuan et al. (2008) confirmed this phenomenon using AOD and CER from MODIS. Using a model simulation, they attributed the positive FAIE over the Gulf region to the influence of slightly soluble organic aerosols and sea salt aerosols, which accounts for higher AOD but delays the activation of small aerosol particles that results in higher CCN and lower CER. However, more detailed analysis is required to explain positive FAIE in China, because previous studies covered a large domain characterized by complex aerosol compositions and varying meteorological conditions, which together may affect the seasonality of cloud systems, aerosol hygroscopic growth, and their correlations.

In this study, FAIE over Eastern China and surrounding waters are examined using aerosol and cloud retrievals from MODIS and meteorological parameters from reanalysis data and in situ measurements. Eastern China is divided into seven sub-sectors with relatively common aerosol properties and meteorological conditions. Coefficients and slopes of the correlation between AOD and low-level liquid cloud effective radius with cloud-top pressure (CTP) greater than 800 hPa are calculated for each region, and the influences of winds and RH on correlations between AOD and CER are analyzed. Datasets used in this study are introduced in Section 2. Results of the study and effects of atmospheric circulations are described in Sections 3 and 4, respectively, and the conclusion and discussion are presented in Section 5.

2. Data and methodology

Daily AOD, CER, and CTP observed by MODIS onboard the Aqua satellite from 2003 to 2012 on 1° × 1° grids are used in this work. For the retrieval of aerosol and cloud properties, MODIS identifies the state of each pixel (clear or cloudy) based on spatial variability (Ackerman et al., 1998). For clear pixels, two independent algorithms are applied to retrieve aerosol properties: the Deep Blue method over land using reflectances at 0.47, 0.66, and 2.13 μm and the dark target method over ocean using seven bands ranging from 0.47 to 2.13 μm (Remer et al., 2005). MODIS Level 2 AOD has a footprint of 10 × 10 km and an overall uncertainty of ±0.05 ± 0.15 τ over land and ±0.03 ± 0.05 τ over ocean (Remer et al., 2005). The Deep Blue algorithm decreases the influence of albedo effects over bright surfaces, thus has high accuracy over land, except over dust and snow surfaces. Thus, our target region does not include Western China, which is desert in Xinjiang and frequently snow covered on the Tibetan Plateau.

By comparison, MODIS retrieves cloud physical and optical properties using 14 spectral bands. Cloud phase (water or ice) is determined based on the distinct differences in absorption at 1.64 μm between water and ice (King et al., 2003). CER is retrieved at 1 × 1 km resolution using absorption at 2.13 μm in combination with information from non-absorbing bands at 0.65, 0.86, and 1.24 μm over land, ocean, and ice surfaces (Platnick et al., 2003).

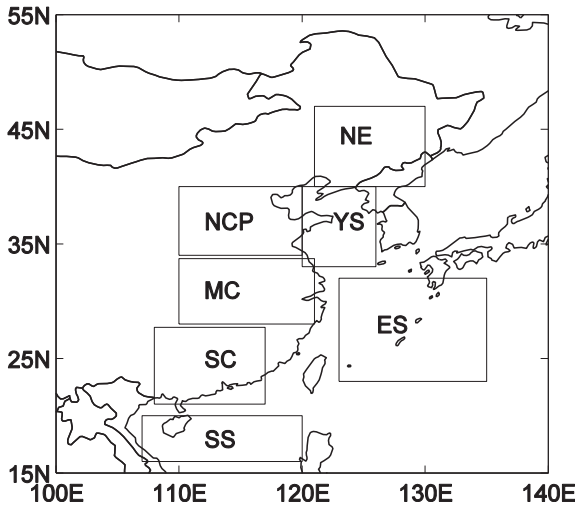

Fig. 1. Regions of Eastern China and surrounding waters analyzed in this study: Northeast China (NE), North China Plain (NCP), Middle China (MC), and South China (SC), Yellow Sea (YS), East Sea (ES) and South China Sea (SS).

Cloud fraction (CF) and cloud-top properties are retrieved at 5 × 5 km resolution using the CO_2-slicing algorithm (Menzel et al., 2003). One of the advantages of the cloud retrieval method of MODIS is that the liquid and ice phases can be distinguished to separate warm and cold clouds. The disadvantage is that MODIS can detect only irradiance reflected by clouds, and thus lacks any effective vertical profiling capability.

With the MODIS algorithm for our study, limitations exist. First, there is uncertainty when using AOD as an indicator of CCN because AOD is related to both the number concentration and aerosol particle size distribution. Some studies have suggested that AI would be better than AOD for representing CCN, because the former decreases the impact of aerosol particle size (Breon et al., 2002; Penner et al., 2012). However, AI is calculated as AOD times the Angstrom exponent, which has no significant correlation with observations from the Aerosol Radiation Network (AERONET) (Levy et al., 2007, 2010). Additionally, a correlation coefficient of 0.98 has been found between AOD and CCN (Andreae, 2009). Recently, AOD has been used at regional scale during a particular season, when variation in aerosol particle size is assumed to be small (Kaufman et al., 2005; Yuan et al., 2008; Koren et al., 2010).

Second, AOD is a column integrated parameter, which may not represent aerosol information at cloud altitude. Costantino and Breon (2013) showed that FAIE estimated with MODIS is more significant when cloud and aerosol are mixed than when decoupled. To limit this effect, we focus on low-level liquid clouds, reported as water cloud phase by MODIS and lower than 2 km as evidenced by CTP greater than 800 hPa. In addition, we use observations from the Aqua satellite, which passes at about 13:30 local time, when the top of the boundary layer is at about 2 km and aerosol particles are generally well mixed (Del Guasta, 2002; Huang et al., 2008; Campbell et al., 2013). To support this assumption, case studies are explored based on MODIS level 2 data and meteorological parameters from special ground sites.

Third, CER are retrieved by irradiance reflected from cloud top, which is dependent on cloud top height and may not represent the average state. To check the possible impact from variations of cloud top height, we binned the cloud top height and calculated correlation between AOD and CER for each thin cloud layer.

Since it is difficult to isolate aerosol and cloud from the background meteorology, we divide Eastern China and the surrounding waters into seven sub-sectors (Fig. 1): Northeast China (NE), North China Plain (NCP), Middle China (MC), and South China (SC), as well as three nearby waters: Yellow Sea (YS), East Sea (ES) and South China Sea (SS). Aerosol chemical composition and meteorological conditions can be considered to be similar in each sector. NCP, MC, and SC are three major polluted regions, while NE is relatively less polluted. MC is centered on the Yangtze River Delta area, and SC includes most of the province of Guangdong and the Pearl River Delta area (Xia, 2010; Zhang et al., 2012). The ocean sectors YS, ES and SS can be affected by pollution through offshore advection. Most of these sectors are affected by the Asian summer monsoon, with a south-to-north shift of the rain belt that causes increased precipitation over SC from May to mid-June, MC from mid-June to mid-July, and the NCP and NE after July (Hu and Ding, 2010). These regions are also affected by the Asian winter monsoon, which induces strong north-westerly winds over NC and north-easterly winds over the Southern China. These synoptic phenomena are associated with the anti-cyclonic circulation of the surface Siberian–Mongolian High (Chang et al., 2004). Compared with northern inland regions, SC and the adjacent ocean are more humid during most seasons due to the Asian Monsoon (Ding and Chan, 2005).

The correlation coefficient between AOD and CER is calculated for each sub-sector based on MODIS level 3 data from 2003 to 2012. To investigate the possible reasons for the observed correlations, this study explores the seasonality of correlations, impact of meteorological factors, and case studies were explored based on MODIS level 2 and level 3 data, daily precipitation observed at 756

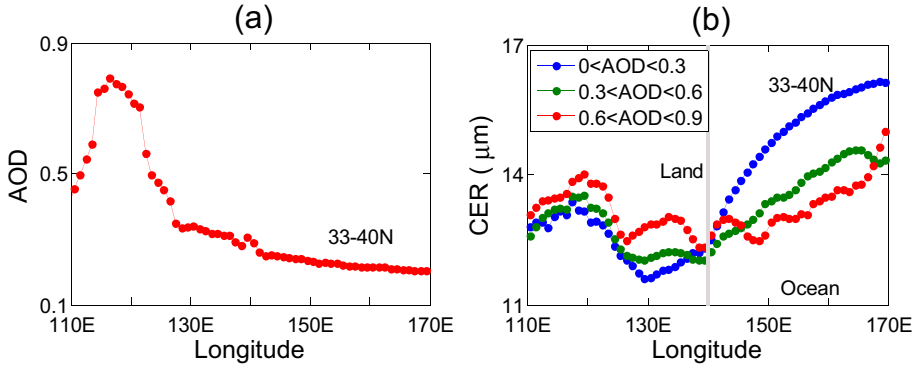

Fig. 2. Longitudinal dependence of aerosol optical depth (AOD) (a), and cloud effective radius (CER) (b) from 110° to 170°E. CER is shown for three intervals of AOD. The dots represent 2003–2012 mean values averaged over 2-degree longitude bins between 33°and 40°N. Both AOD and CER are from MODIS Aqua level 3 daily mean data. The gray vertical line in panel (b) represents the position of the coast.

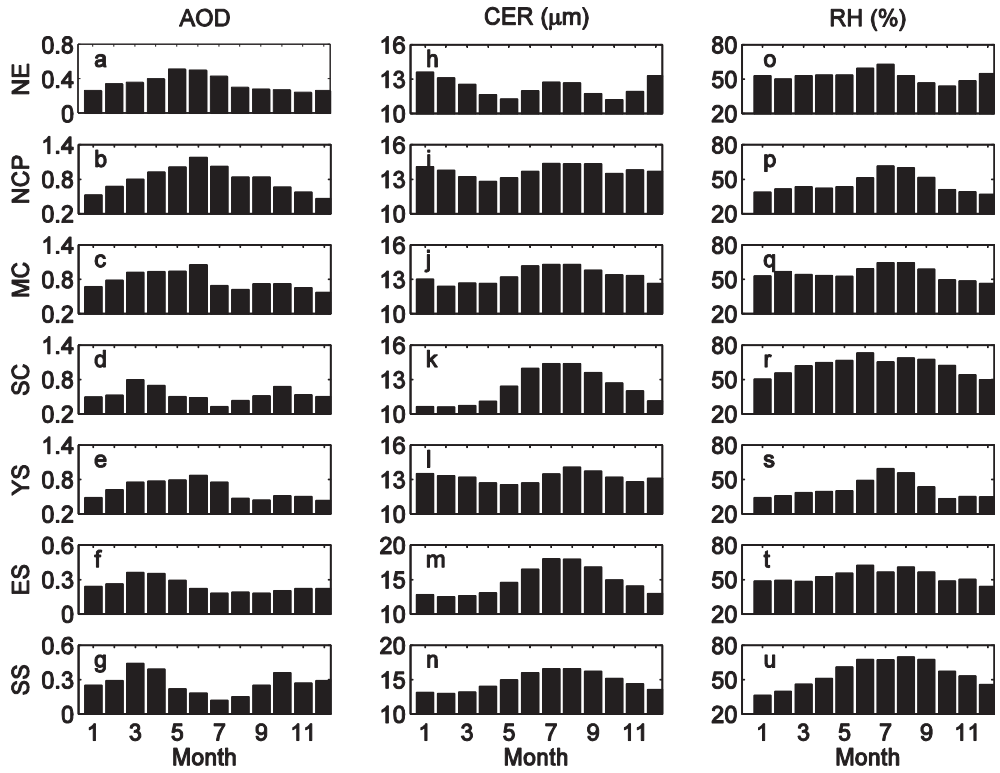

Fig. 3. Monthly mean values of AOD, CER (μm) and relative humidity (RH, %) over the seven regions of Eastern China. AOD and CER are from MODIS, as in Fig. 2. RH is from ECMWF reanalysis data.

meteorological stations in China, and daily RH and wind speed at a resolution of 1.5° × 1.5° from ECMWF reanalysis during 2003–2012. The topographic data from the National Geophysical Data Center (NGDC) are also employed in the study. Each of the datasets is interpolated or aggregated to a common 1° × 1° grid that matches that of MODIS Level 3 data.

3. Results

3.1. Variation in CER with AOD over the North Pacific

The meridional mean of CER and AOD is calculated between 33°N and 40°N from 2003 to 2012, with resolution of 1° × 1°. The average AOD peaks at 0.8 near 118°E between 110°E to 170°E (Fig. 2a). For the open ocean, east of 140°E, AOD decreases from prominent aerosol source region to relatively clean area with mean AOD < 0.3.

According to the range of regional AOD, three types of pollution conditions are defined: low (0–0.3), moderate (0.3–0.6), and high (0.6–0.9). The meridional means of CER for the three AOD intervals are shown in Fig. 2b. For the regions west of 140°E, CER peaks at 14 μm near 118°E (Fig. 2b) and exhibits variation similar to that in AOD. Over this land region, CER for high-pollution conditions is 0.5–1 μm higher than that for relatively clean conditions. For the regions east of 140°E, CER increases steadily from 12 to 16 μm with longitude, a trend opposite to that of AOD. Over this open-ocean region, CER for high-pollution conditions is 1–2 μm smaller than that for relatively clean conditions. Kaufman

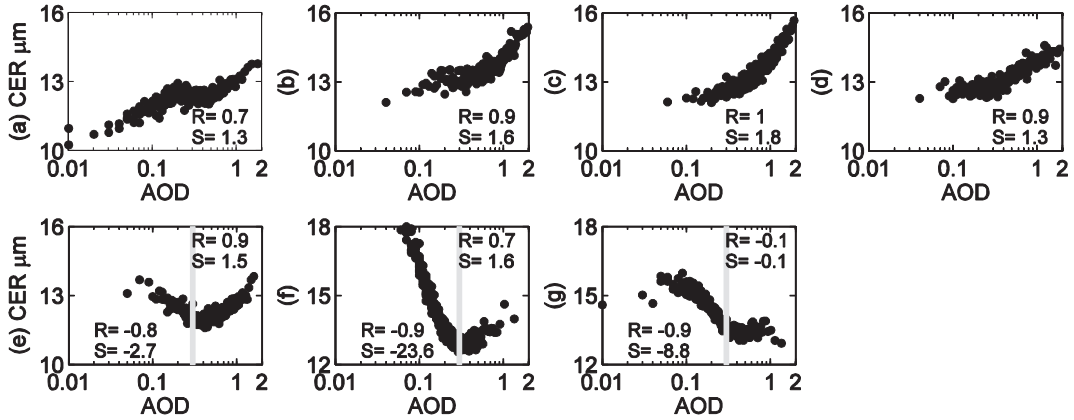

Fig. 4. Correlations between CER and AOD over seven regions in Eastern China. Data are from MODIS, as in Fig. 2. Observations with cloud top pressure less than 800 hPa or topography greater than 600 m are excluded. The points show CER sorted by AOD, and both AOD and CER are averaged over every 300 data points. *R* represents the correlation coefficient between CER and AOD, and S represents the regression slope.

et al. (2005) reported variations in CER with AOD and longitude over the Atlantic. They found a decreasing trend of CER with increasing AOD, a result similar to ours over the open ocean. The positive relationship between CER and AOD over the land (Fig. 2b), however, indicates that other processes are likely counteracting the Twomey effect.

3.2. Monthly mean of AOD and CER

Fig. 3 shows monthly mean level of AOD, CER, and RH for each sub-region. Over the urban continental region, including NE, the NCP, and MC, peak values of AOD occur in June (Fig. 3a–c), likely due to hygroscopic anthropogenic particles (Wang et al., 2008). AOD over the YS exhibits monthly variation similar to that of the urban regions, because it is frequently influenced by pollutants from nearby urban areas. Over these regions, AOD is also high in spring when strong dust storms persist (Husar et al., 2001). AODs over SC, the ES, and the SS reach a maximum in spring (Fig. 3d–g). However, this is likely due to transported pollution originated from local agricultural burning in Southeast Asia (Sang et al., 2011). For the period of 2003–2012, the annual mean AOD exceeds 0.5 for the NCP, MC, and SC. AOD is generally lower than 0.3 over the ES and SS.

Large values of CER are shown, in both winter and summer, over NE, the NCP, and the YS (Fig. 3h–n). However, only one CER peak in summer is found from the other regions. Annual mean CER exceeds 14 μm over the ES and SS, but it is less than 14 μm in other regions. The monthly mean of RH shows similar variations with CER, with a correlation coefficient ranging from 0.22 to 0.96 (Fig. 3o–u). By comparison, RH shows variations similar to those in AOD over NE, the NCP, MC, and the YS. However, it shows variations opposite to those in AOD over the ES and SS.

3.3. Correlations between AOD and CER

Several steps were taken before we calculated correlations between AOD and CER. First, data for elevations higher than 600 m above sea level were excluded to eliminate the potential influence of topography. Second, because rain can affect both aerosol and cloud properties, land grid cells with precipitation were excluded using the total precipitation observed at the meteorological sites. Third, following the approach of Koren et al. (2008), all cells with available observations of both AOD and CER were selected and grouped by AOD. The pairs of AOD and CER were then averaged for every 300 sorted cells.

Fig. 4 shows the correlation between AOD and CER in each sub-region. Negative correlation coefficients of −0.8 to −0.9 occur for AOD smaller than 0.3 over SC, the SS, and the ES (Fig. 4e–g). However, positive correlations occur over SC and the ES when AOD is higher than 0.3. In contrast, urban continental areas and nearby waters, including NE, the NCP, MC, and the YS show positive correlations between AOD and CER ranging from 0.7 to 0.99 (Fig. 4a–d).

The slope of the regressions between CER and AOD can be used to represent the magnitude of FAIE. Slopes range from −2.7 to −23.6 for AOD < 0.3 over SC, the SS, and the ES (Fig. 4e–g). In contrast, slopes of 1.3–1.8 are shown over NE, the NCP, MC, and the YS (Fig. 4a–d).

3.4. Seasonality of correlations between AOD and CER

The negative correlation between AOD and CER over the ES and the positive correlation over the NCP are both statistically significant. The seasonal variations of such correlations for these regions during 2003–2012 were analyzed (Fig. 5). In the NCP, significant

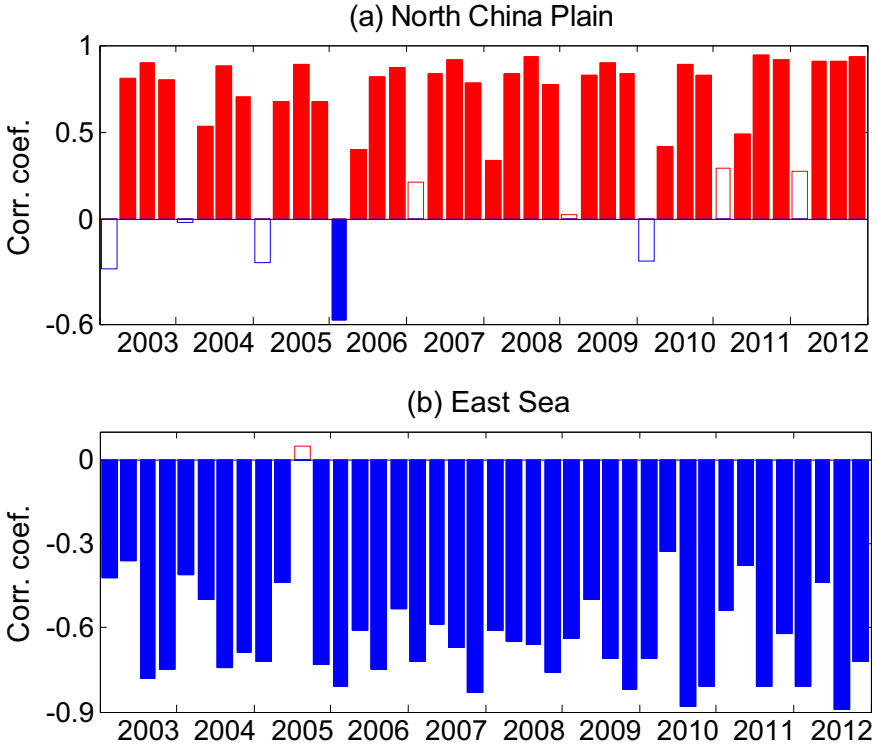

Fig. 5. Seasonality of the correlation between AOD and CER over the North China Plain and the East Sea. The data and method are as in Fig. 4. For each year, the sequence of the bars runs from winter (January, February and December of the previous year) to autumn (August, September and November). The solid bars represent statistically significant correlations ($p < 0.05$), and the empty bars denote insignificant correlation.

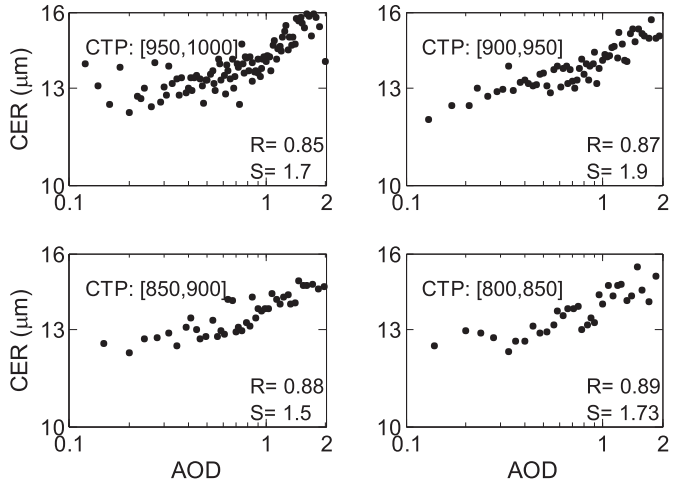

Fig. 6. Correlation coefficients between AOD and CER over North China Plain binned by AOD. Each panel show the correlation for a different interval of cloud top pressure (CTP). The data and method are described in Fig. 4.

positive correlations between 0.34 and 0.93 ($p < 0.05$) are shown from spring to fall. During most winters, the correlations are either negative or weakly positive, depending on the year. Over the ES, significant negative correlations between AOD and CER occur for all seasons except the summer of 2005. During this period, the correlation is positive for some high-pollution days with AOD greater than 0.3, indicating outflow from the continent.

4. Effect of atmospheric circulation

4.1. Positive FAIE in previous studies

Positive FAIE has been observed in previous studies. Myhre et al. (2007) attributed the positive indirect effect observed in the Mediterranean Sea to associated changes in CTP. They hypothesized that as CTP decreases, AOD and CER increase, thus weakening the positive correlation between AOD and CER when CTP is large. To test this hypothesis, CTP has been divided into four sub-intervals from 800 hPa to 1000 hPa, with a depth of 50 hPa. Correlations between AOD and CER for each interval were calculated over NCP. Similar positive correlations between AOD and CER are still found for each sub-interval (Fig. 6), indicating that changes in CTP may not be the only reason to explain the positive FAIE over China mainland.

Yuan et al. (2008) also revealed positive correlations between AOD and CER over the Gulf of Mexico and Eastern China, which they considered to be related to the effects of slightly soluble organics particles (SSO) and giant cloud condensation nuclei (CCN). Using the 2-D Goddard Cumulus Ensemble model and Twomey theory, Yuan et al. (2008) explained that such particles can contribute to large AOD but fewer total cloud droplets and thus higher CER. Since most SSO are hydrophobic and not easily activated, giant CCN preferentially absorb water vapor due to their lower critical supersaturation, resulting in the deactivation of many small aerosol particles (Rosenfeld et al., 2002). However, most giant CCN are generated from sea salt aerosols or mixed mineral dust and soluble aerosols (Levin et al., 1996). Concentrations of sea salt aerosols are

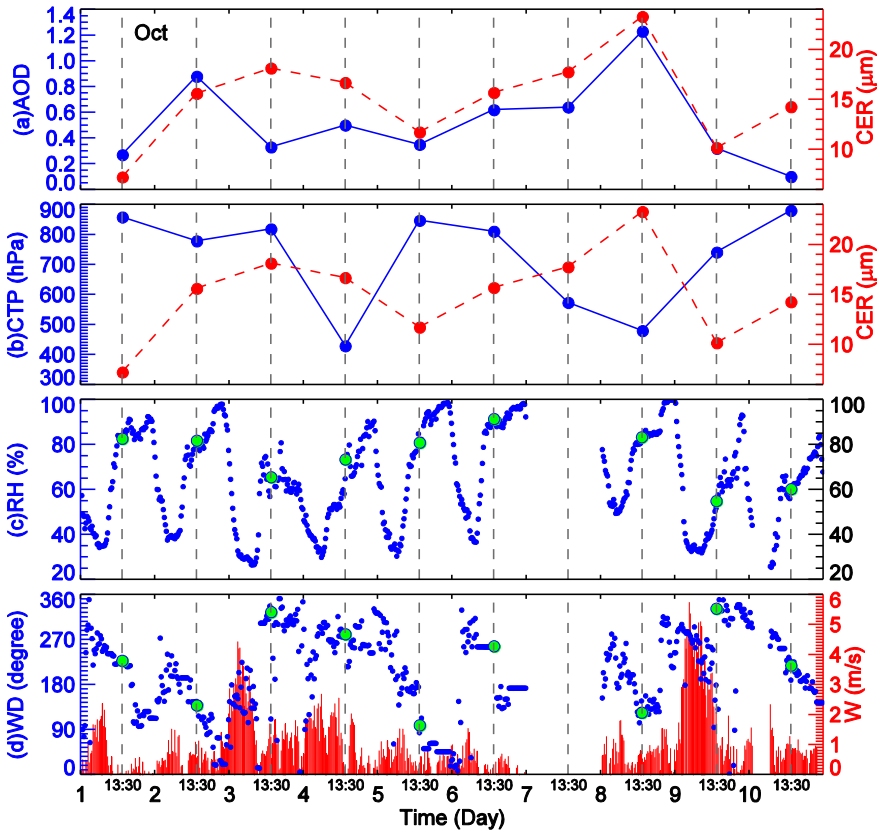

Fig. 7. (a) Daily variation of AOD and CER, (c) relative humidity (RH) and (d) wind fields around Xianghe (39.5°N, 116.6°E) from 1 October to 10 October in 2012. AOD and CER are MODIS level 2 data, measured at about 13:30 local time and are averaged over the region defined by 38.5–40.5°N and 115.5–117.5°E. RH and wind speed (W) are observed at the Xianghe site, with a time resolution of 5 min. Green circles are observations at 13:30. Wind direction (WD) is represented by values from 0 to 360°, with northerly wind represented by 0°.

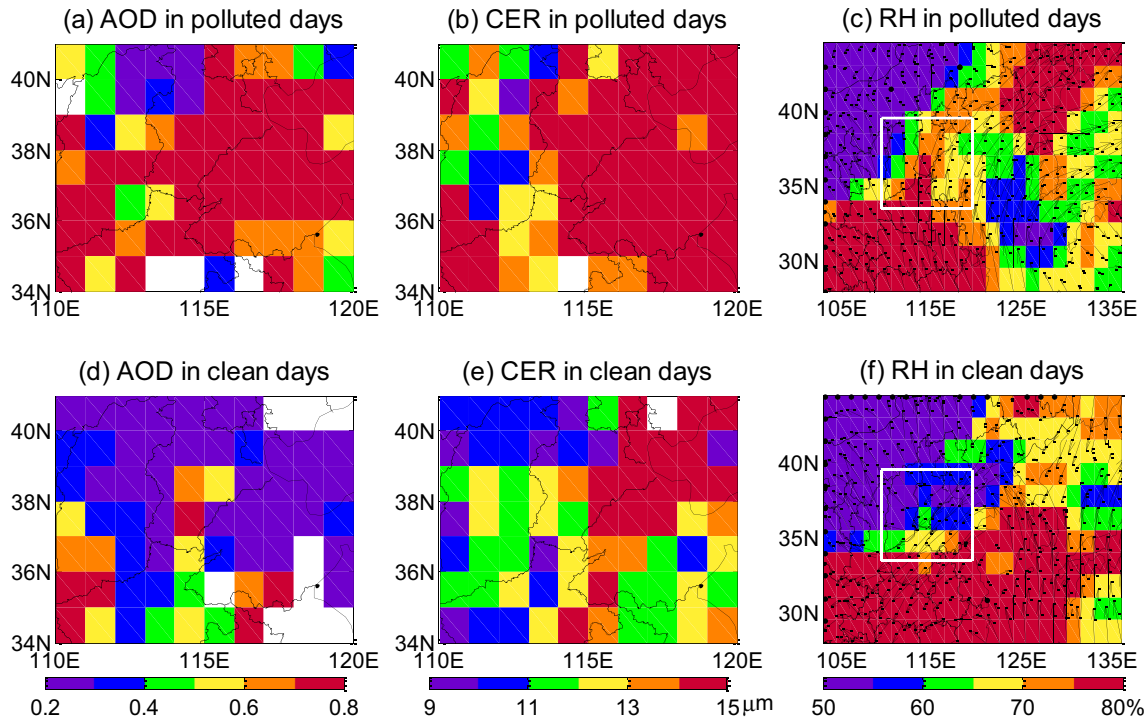

Fig. 8. Spatial distribution of AOD, CER, wind fields, and RH at 850 hPa for polluted days and clean days in August 2005 over the North China Plain. AOD and CER are from MODIS, as in Fig. 2. Wind speed and RH are ECMWF reanalysis data. White pixels represent regions where no simultaneous observations of AOD and CER were made. The wind speed and RH are shown on a larger domain than are AOD and CER. The white box in panels (c) and (f) shows the North China Plain, the domain for the other four panels.

small over inland China, and the activation rate of dust aerosols is uncertain (Kelly et al., 2007; Zhang et al., 2012). In addition, SSO accounts for only about 15% of the total aerosol mass in China (Zhang et al., 2012). Thus, the hypothesis proposed by Yuan et al. (2008) may not be sufficient to account for the observed positive FAIE in Eastern China.

4.2. Case study of the positive effect over Xianghe

The apparent evidence of positive FAIE over inland areas is also observed on a daily time scale. To investigate daily relationships between AOD and CER, we selected a period, 1 October to 10 October in 2012, with frequent changes in atmospheric circulation

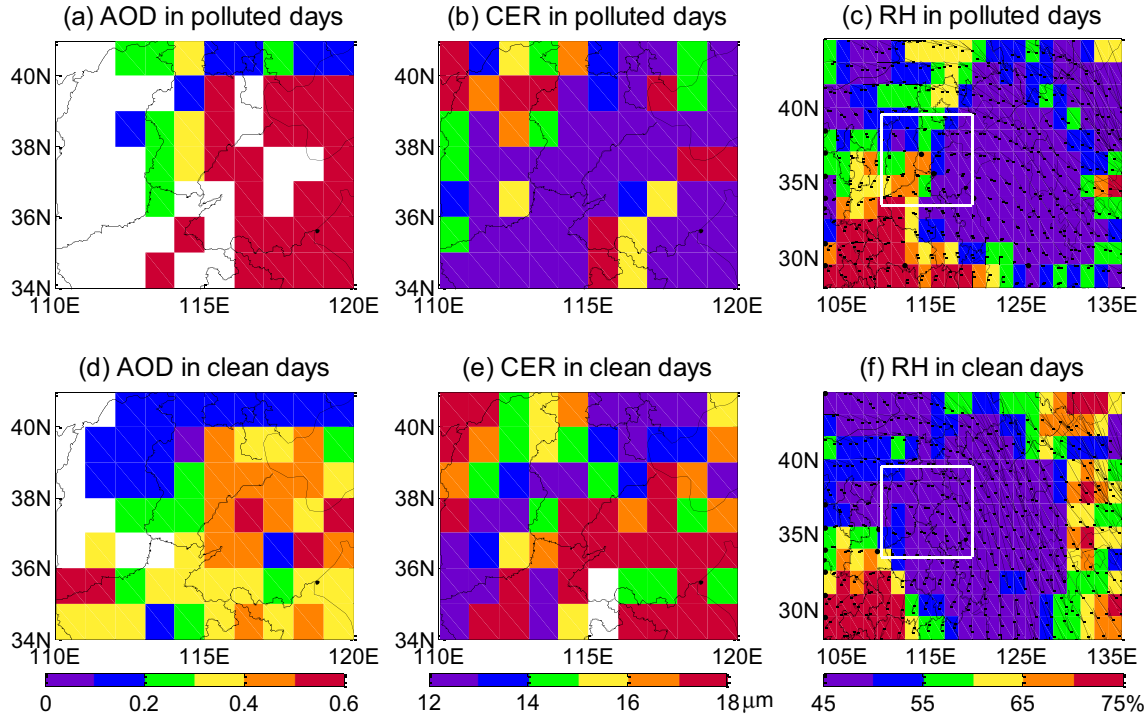

Fig. 9. Same as Fig. 8 but for January 2006.

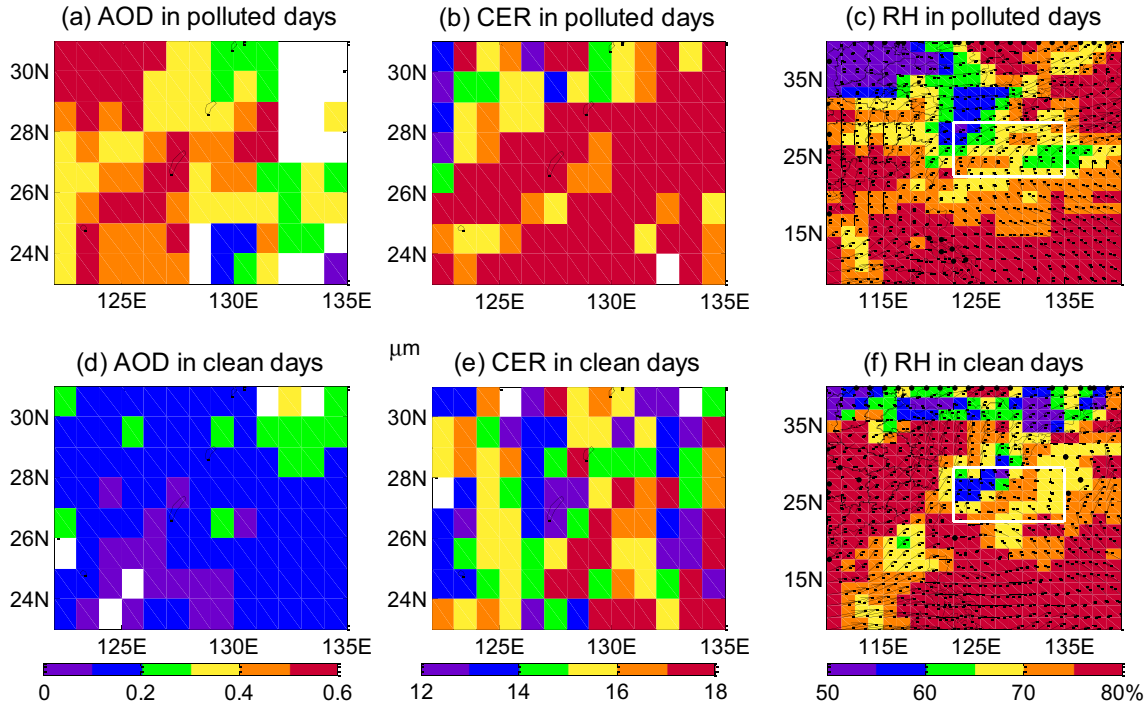

Fig. 10. Same as Fig. 8 but for summer 2005 over the East Sea. The white box in panels (c) and (f) shows the East Sea, the domain for the other four panels.

over Xianghe (39.5°N, 116.6°E) (Fig. 7), which is in the NCP. During this period, the average AOD is more than 0.5, and maximum values reach as high as 1.2. On polluted days, such as 2 and 8 October, weak and southerly winds prevail. In contrast, clean days, such as 1, 3, and 9 October, are characterized by strong and northerly winds. The daily variations in AOD and CER are associated with dramatic variations in wind speed, wind direction, and RH. For example, conditions at 13:30 on 8 October are southerly wind of less than 2 m s^{-1} and RH of 83%; however, during the entire morning of 9 October, the wind is northerly, with speed of 4–5 m s^{-1} and correspondingly smaller RH of 52%. The change in the wind field and RH may have contributed to the sharp decrease in AOD and CER.

4.3. *Effects of atmospheric circulation on FAIE over the NCP*

Both the monthly variation and the case study show that both RH and wind fields correlate with AOD and CER (Figs. 3 and 7). Such effects of RH and wind fields have also been demonstrated in previous studies (Koren et al., 2010; Wang et al., 2010, 2011). Therefore, it is important to consider the question of whether the positive correlation between AOD and CER observed over inland China regions can be related to atmospheric circulation. Fig. 5 shows that positive FAIE usually appears in summer in the NCP. As a result, possible effects of atmospheric circulation on regional aerosol–cloud relationships are investigated during August 2005. AOD, CER, as well as the corresponding weather conditions for the top five most-polluted and cleanest days of this month are shown in Fig. 8.

On polluted days, AOD exceeds 0.6 on average (Fig. 8a) and CER is greater than 14 μm (Fig. 8b). In contrast, smaller values of AOD, 0–0.4, are observed on clean days (Fig. 8d), with most CER values being less than 12 μm (Fig. 8e). The higher values of AOD and CER on polluted days are consistent with southerly winds prevailing, which likely advect aerosol particles and abundant water vapor from southern China. On clean days, northeast winds prevail, bringing cleaner and drier air from northern China. This effect can also be seen from emission inventories (Li et al., 2007).

A positive correlation between AOD and CER exists over the NCP during most seasons, except for some winter periods; As Fig. 5 shows, a significant negative correlation occurs in early 2006. The distributions of AOD and CER relative to atmospheric circulations

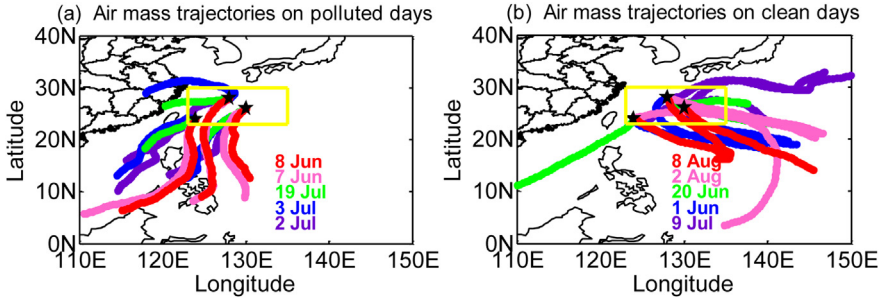

Fig. 11. Air mass back trajectories on (a) five polluted days and (b) five clean days in summer 2005 over the East Sea (yellow box). The back trajectories are simulated by the Hybrid Single Particle Lagrangian Integrated Trajectory Model for three points; 24°N,124°E; 28°N, 128°E; and 26°N, 130°E.

are examined for relatively polluted and clean days of January 2006, as shown in Fig. 9. Compared with clean days, the regional mean AOD during pollution episodes is higher by 0.3, and the CER is lower by 1.5 μm. However, in both cases, the background circulation shows a similar pattern, with northwesterly wind and low RH. This result indicates that the Twomey effect can be observed over land when the wind fields and spatial distribution of RH show little variation.

4.4. Effects of atmospheric circulation on FAIE over the ES

In contrast to the dominant positive FAIE observed over inland regions, correlations between AOD and CER over the ES are usually negative (Fig. 5b). However, a positive correlation occurs when AOD is higher than 0.3 (Fig. 10b), especially for the summer of 2005 (Fig. 5b). During the top five polluted days, high levels of pollutants (Fig. 10a) are transported from Southeast Asia by southwesterly wind (Figs. 10c and 11a). This prevailing flow carries abundant water vapor, which enhances local CER (Fig. 10b). Such pollution episodes are characterized by AOD greater than 0.4 and CER higher than 17 μm. In contrast, for the five cleanest days in summer, AOD is 0.15 and CER is 15.5 μm on average (Fig. 10d). Winds on these days are southeasterly, bringing clean air from a subtropical high to the ES area (Figs. 10f and 11b).

5. Conclusions and discussion

The first aerosol indirect effect (FAIE) over Eastern China was studied for the time period of 2003–2012 by examining correlations between cloud effective radius (CER) and aerosol optical depth (AOD) using Moderate Resolution Imaging Spectroradiometer (MODIS) observations. Eastern China was divided into seven regions for the study according to meteorological conditions and air pollution situation, which are four inland regions: Northeast China (ES), North China Plain (NCP), Middle China (MC), and South China (SC), as well as three nearby waters: Yellow Sea (YS), East Sea (ES) and South China Sea (SS). Significant positive correlations between CER and AOD were found over inland regions and the YS, while negative correlations consistent to Twomey effect was observed over the ES and SS for AOD smaller than 0.3. However, negative FAIE over the ocean regions weakened significantly when AOD was higher than 0.3. The magnitude of FAIE varied with season. For the NCP and SC, positive correlation between CER and AOD was found for most seasons, except during spring or winter of some years. For the ES, negative FAIE dominated.

Positive FAIE observed over Eastern China is likely attributable to meteorological influence. During pollution episodes, the atmospheric circulation usually favors transport of both pollutants and water vapor from SC or Southeast Asia, leading to simultaneous increases in both AOD and CER. In contrast, dry and relatively clean northerly winds or anticyclonic circulation prevailed on clear days. Both effects contribute to simultaneous variations in AOD and CER. In summary, the Twomey effect was observed over both land and ocean in China, but positive FAIE also occurred over land when meteorological conditions were favorable.

A major uncertainty in our study is the assumption that AOD can be used to represent CCN. First, aerosol and cloud properties from MODIS are retrieved from space. Horizontally, aerosol properties were assumed uniform within $1^\circ \times 1^\circ$ resolved grids. Vertically, AOD represents the total column aerosol, but cloud properties are highly sensitive to CCN at the cloud base. To limit this effect, we focus on low-level liquid clouds, reported as water cloud phase by MODIS and lower than 2 km as evidenced by CTP greater than 800 hPa. Second, AOD may not correlate with aerosol particle number because AOD is also sensitive to the size and absorbing properties of particles (Hoppel et al., 1990; Steele and Hamill, 1981).

Another possible source of uncertainty is associated with the influence of meteorology on aerosol–cloud interactions. Our study showed that both AOD and cloud properties were correlated with relative humidity and wind field, but it is not possible to isolate observed aerosol and cloud properties from background meteorological conditions.

Despite these limitations, this study provides a general description of the aerosol first indirect effect over Eastern China and the adjacent ocean. Positive correlations between AOD and CER are found over the mainland, which can be attributed in part to the influence of general circulation. Our results suggest that the effect of meteorology may not be negligible when investigating the aerosol indirect effect on a large scale, especially when the weather conditions are complex and change frequently. An interactive cloud–climate model may help diagnose and quantify the impacts of aerosol on cloud droplets under variable meteorological conditions.

Acknowledgment

The authors would like to thank Liang Ran and Yong Wang for their suggestions. We also thank the two anonymous reviewers for helping to improve the manuscript. This work is jointly supported by the “Strategic Priority Research Program” of the Chinese Academy of Sciences (Grant No. XDA05100000), National Basic Research Program of China (Grant No. 2013CB955800), and National Natural Science Foundation of China (Grant No. 41175030).

References

Ackerman, S.A., Strabala, K.I., Menzel, W.P., Frey, R.A., Moeller, C.C., Gumley, L.E., 1998. Discriminating clear sky from clouds with MODIS. J. Geophys. Res. 103, 32,141–32,157. http://dx.doi.org/10.1029/1998JD200032.

Andreae, M.O., Rosenfeld, D., Artaxo, P., Costa, A.A., Frank, G.P., Longo, K.M., Silva-Dias, M.A.F., 2004. Smoking rain clouds over the Amazon. Science 303, 1337–1342. http://dx.doi.org/10.1126/science.1092779.

Andreae, M.O., 2009. Correlation between cloud condensation nuclei concentration and aerosol optical thickness in remote and polluted regions. Atmos. Chem. Phys. 9, 543–556.

Breon, F.M., Tanre, D., Generoso, S., 2002. Aerosol effect on cloud droplet size monitored from satellite. Science 295, 834–838. http://dx.doi.org/10.1126/science.1066434.

Campbell, J.R., Reid, J.S., Westphal, D.L., Zhang, J., Tackett, J.L., Chew, B.N., Welton, E.J., Shimizu, A., Sugimoto, N., Aoki, K., 2013. Characterizing the vertical profile of aerosol particle extinction and linear depolarization over Southeast Asia and the Maritime Continent: the 2007–2009 view from CALIOP. Atmos. Res. 122, 520–543.

Chang, C.P., Wang, Z., Ju, J.H., Li, T., 2004. On the relationship between western maritime continent monsoon rainfall and ENSO during northern winter. J. Clim. 17, 665–672. http://dx.doi.org/10.1175/1520-0442(2004)017<0665:otrbwm>2.0.co;2.

Chen, Y., Penner, J.E., 2005. Uncertainty analysis for estimates of the first indirect aerosol effect. Atmos. Chem. Phys. 5, 2935–2948.

Costantino, L., Breon, F.M., 2013. Aerosol indirect effect on warm clouds over South-East Atlantic, from co-located MODIS and CALIPSO observations. Atmos. Chem. Phys. 13, 69–88. http://dx.doi.org/10.5194/acp-13-69-2013.

Del Guasta, M., 2002. Daily cycles in urban aerosols observed in Florence (Italy) by means of an automatic 532–1064 nm LIDAR. Atmos. Environ. 36, 2853–2865. http://dx.doi.org/10.1016/s1352-2310(02)00136-x.

Ding, Y.H., Chan, J.C.L., 2005. The East Asian summer monsoon: an overview. Meteorol. Atmos. Phys. 89, 117–142. http://dx.doi.org/10.1007/s00703-005-0125-z.

Dusek, U., Frank, G.P., Hildebrandt, L., Curtius, J., Schneider, J., Walter, S., Chand, D., Drewnick, F., Hings, S., Jung, D., Borrmann, S., Andreae, M.O., 2006. Size matters more than chemistry for cloud-nucleating ability of aerosol particles. Science 312, 1375–1378. http://dx.doi.org/10.1126/science.1125261.

Feingold, G., Remer, L., Ramaprasad, J., Kaufman, Y., 2001. Analysis of smoke impact on clouds in Brazilian biomass burning regions: an extension of Twomey's approach. J. Geophys. Res. 106, 22907–22922.

Feingold, G., Eberhard, W., Veron, D., Previdi, M., 2003. First measurements of the Twomey indirect effect using ground-based remote sensors. Geophys. Res. Lett. 30, 1287. http://dx.doi.org/10.1029/2001JD000732.

Hoppel, W.A., Fitzgerald, J.W., Frick, G.M., Larson, R.E., Mack, E.J., 1990. Aerosol size distributions and optical-properties found in the marine boundary-layer over the Atlantic-Ocean. J. Geophys. Res. Atmos. 95, 3659–3686.
Hu, Y.M., Ding, Y.H., 2010. Simulation of 1991-2005 Meiyu seasons in the Yangtze–Huaihe region using BCC_RegCM 1.0. Chin. Sci. Bull. 55, 1077–1083. http://dx.doi.org/10.1007/s11434-009-0473-z.
Huang, J., Lin, B., Minnis, P., Wang, T., Wang, X., Hu, Y., Yi, Y., Ayers, J.K., 2006. Satellite-based assessment of possible dust aerosols semi-direct effect on cloud water path over East Asia. Geophys. Res. Lett. 33.
Huang, J., Zhang, W., Zuo, J., Bi, J., Shi, J., Wang, X., Chang, Z., Huang, Z., Yang, S., Zhang, B., 2008. An overview of the semi-arid climate and environment research observatory over the Loess Plateau. Adv. Atmos. Sci. 25, 906–921.
Husar, R.B., Tratt, D., Schichtel, B., Falke, S., Li, F., Jaffe, D., Gasso, S., Gill, T., Laulainen, N.S., Lu, F., 2001. Asian dust events of April 1998. J. Geophys. Res. 106, 18317–18330. http://dx.doi.org/10.1029/2000JD900788.
Kaufman, Y.J., Koren, I., Remer, L.A., Rosenfeld, D., Rudich, Y., 2005. The effect of smoke, dust, and pollution aerosol on shallow cloud development over the Atlantic Ocean. Proc. Natl. Acad. Sci. U. S. A. 102, 11207–11212. http://dx.doi.org/10.1073/pnas.0505191102.
Kelly, J.T., Chuang, C.C., Wexler, A.S., 2007. Influence of dust composition on cloud droplet formation. Atmos. Environ. 41, 2904–2916. http://dx.doi.org/10.1016/j.atmosenv.2006.12.008.
King, M.D., Menzel, W.P., Kaufman, Y.J., Tanre, D., Gao, B.C., Platnick, S., Ackerman, S.A., Remer, L.A., Pincus, R., Hubanks, P.A., 2003. Cloud and aerosol properties, precipitable water, and profiles of temperature and water vapor from MODIS. IEEE Trans. Geosci. Remote Sens. 41, 442–458. http://dx.doi.org/10.1109/tgrs.2002.808226.
Koren, I., Martins, J.V., Remer, L.A., Afargan, H., 2008. Smoke invigoration versus inhibition of clouds over the Amazon. Science 321, 946–949. http://dx.doi.org/10.1126/science.1159185.
Koren, I., Feingold, G., Remer, L.A., 2010. The invigoration of deep convective clouds over the Atlantic: aerosol effect, meteorology or retrieval artifact? Atmos. Chem. Phys. 10, 8855–8872 http://dx.doi.org/10.5194/acp-10-8855-2010.
Levin, Z., Ganor, E., Gladstein, V., 1996. The effects of desert particles coated with sulfate on rain formation in the eastern Mediterranean. J. Appl. Meteorol. 35, 1511–1523. http://dx.doi.org/10.1175/1520-0450(1996)035<1511:teodpc>2.0.co;2.
Levy, R.C., Remer, L.A., Mattoo, S., Vermote, E.F., Kaufman, Y.J., 2007. Second-generation operational algorithm: retrieval of aerosol properties over land from inversion of moderate resolution imaging spectroradiometer spectral reflectance. J. Geophys. Res. Atmos. 112. http://dx.doi.org/10.1029/2006jd007811. D1321.
Levy, R.C., Remer, L.A., Kleidman, R.G., Mattoo, S., Ichoku, C., Kahn, R., Eck, T.F., 2010. Global evaluation of the Collection 5 MODIS dark-target aerosol products over land. Atmos. Chem. Phys. 10, 10399–10420. http://dx.doi.org/10.5194/acp-10-10399-2010.
Li, C., Marufu, L.T., Dickerson, R.R., Li, Z., Wen, T., Wang, Y., Wang, P., Chen, H., Stehr, J.W., 2007. In situ measurements of trace gases and aerosol optical properties at a rural site in northern China during East Asian Study of Tropospheric Aerosols: an International Regional Experiment 2005. J. Geophys. Res. Atmos. 1984–2012, 112.
Loeb, N.G., Schuster, G.L., 2008. An observational study of the relationship between cloud, aerosol and meteorology in broken low-level cloud conditions. J. Geophys. Res.-Atmos., 113. http://dx.doi.org/10.1029/2007jd009763. D14214.
Lohmann, U., Lesins, G., 2002. Stronger constraints on the anthropogenic indirect aerosol effect. Science 298, 1012. http://dx.doi.org/10.1126/science.1075405.
Lohmann, U., Feichter, J., 2005. Global indirect aerosol effects: a review. Atmos. Chem. Phys. 5, 715C737.
Mauger, G.S., Norris, J.R., 2007. Meteorological bias in satellite estimates of aerosol-cloud relationships. Geophys. Res. Lett. 34. http://dx.doi.org/10.1029/2007gl029952. L16824.
Menzel, W.P., Wylie, D.P., Jackson, D., Bates, J.J., 2003. HIRS observations of clouds since 1978. In: Menzel, W.P., Zhang, W.J., LeMarshall, J., Tokuno, M. (Eds.), Applications with Weather Satellites, Proceedings of the Society of Photo-optical Instrumentation Engineers (Spie), pp. 55–62.
Myhre, G., Stordal, F., Johnsrud, M., Kaufman, Y.J., Rosenfeld, D., Storelvmo, T., Kristjansson, J.E., Berntsen, T.K., Myhre, A., Isaksen, I.S.A., 2007. Aerosol-cloud interaction inferred from MODIS satellite data and global aerosol models. Atmos. Chem. Phys. 7, 3081–3101.
Nakajima, T., Higurashi, A., Kawamoto, K., Penner, J.E., 2001. A possible correlation between satellite-derived cloud and aerosol microphysical parameters. Geophys. Res. Lett. 28, 1171–1174. http://dx.doi.org/10.1029/2000GL012186.
Nenes, A., Charlson, R.J., Facchini, M.C., Kulmala, M., Laaksonen, A., Seinfeld, J.H., 2002. Can chemical effects on cloud droplet number rival the first indirect effect? Geophys. Res. Lett. 29 http://dx.doi.org/10.1029/2002gl015295, 1848.
Penner, J.E., Zhou, C., Xu, L., 2012. Consistent estimates from satellites and models for the first aerosol indirect forcing. Geophys. Res. Lett. 39. http://dx.doi.org/10.1029/2012gl051870. L13810.
Platnick, S., King, M.D., Ackerman, S.A., Menzel, W.P., Baum, B.A., Riedi, J.C., Frey, R.A., 2003. The MODIS cloud products: algorithms and examples from Terra. IEEE Trans. Geosci. Remote Sens. 41, 459–473. http://dx.doi.org/10.1109/tgrs.2002.808301.
Quaas, J., Boucher, O., Lohmann, U., 2006. Constraining the total aerosol indirect effect in the LMDZ and ECHAM4 GCMs using MODIS satellite data. Atmos. Chem. Phys. 6, 947–955.
Ramanathan, V., Crutzen, P.J., Kiehl, J.T., Rosenfeld, D., 2001. Atmosphere – aerosols, climate, and the hydrological cycle. Science 294, 2119–2124.
Remer, L.A., Kaufman, Y.J., Tanre, D., Mattoo, S., Chu, D.A., Martins, J.V., Li, R.R., Ichoku, C., Levy, R.C., Kleidman, R.G., Eck, T.F., Vermote, E., Holben, B.N., 2005. The MODIS aerosol algorithm, products, and validation. J. Atmos. Sci. 62, 947–973. http://dx.doi.org/10.1175/JAS3385.1.
Rosenfeld, D., Lahav, R., Khain, A., Pinsky, M., 2002. The role of sea spray in cleansing air pollution over ocean via cloud processes. Science 297, 1667–1670. http://dx.doi.org/10.1126/science.1073869.
Sang, X.U.E.F., Chan, C.Y.U., Engling, G., Chan, L.O.Y.I.N., Wang, X.U.E.M.E.I., Zhang, Y.I.N.A.N., Shi, S., Zhang, Z.H.I.S., Zhang, T., Hu, M., 2011. Levoglucosan enhancement in ambient aerosol during springtime transport events of biomass burning smoke to Southeast China. Tellus B 63, 129–139.
Sekiguchi, M., Nakajima, T., Suzuki, K., Kawamoto, K., Higurashi, A., Rosenfeld, D., Sano, I., Mukai, S., 2003. A study of the direct and indirect effects of aerosols using global satellite data sets of aerosol and cloud parameters. J. Geophys. Res. 108. http://dx.doi.org/10.1029/2002JD003359.
Steele, H.M., Hamill, P., 1981. Effects of temperature and humidity on the growth and optical properties of sulphuric acid—water droplets in the stratosphere[J]. J. Aerosol Sci. 12 (6), 517–528.
Twomey, S., 1977. The influence of pollution on the shortwave albedo of clouds. J. Atmos. Sci. 34, 1149–1152.
Wang, J., Lee, Y.N., Daum, P.H., Jayne, J., Alexander, M.L., 2008. Effects of aerosol organics on cloud condensation nucleus (CCN) concentration and first indirect aerosol effect. Atmos. Chem. Phys. 8, 6325–6339.
Wang, X., Huang, J., Zhang, R., Chen, B., Bi, J., 2010. Surface measurements of aerosol properties over northwest China during ARM China 2008 deployment. J. Geophys. Res. Atmos. 1984–2012, 115.
Wang, Y.S., Xin, J.Y., Li, Z.Q., Wang, S.G., Wang, P.C., Hao, W.M., Nordgren, B.L., Chen, H.B., Wang, L.L., Sun, Y., 2011. Seasonal variations in aerosol optical properties over China. J. Geophys. Res.-Atmos. 116. http://dx.doi.org/10.1029/2010jd015376. D18209.
Warner, J., Twomey, S., 1967. Production of cloud nuclei by cane fires and effect on cloud droplet concentration. J. Atmos. Sci. 24, 704. http://dx.doi.org/10.1175/1520-0469(1967)024<0704:tpocnb>2.0.co;2.
Xia, X.A., 2010. Spatiotemporal changes in sunshine duration and cloud amount as well as their relationship in China during 1954–2005. J. Geophys. Res.-Atmos. 115. http://dx.doi.org/10.1029/2009jd012879. D00k06.
Yuan, T.L., Li, Z.Q., Zhang, R.Y., Fan, J.W., 2008. Increase of cloud droplet size with aerosol optical depth: an observation and modeling study. J. Geophys. Res. 113. http://dx.doi.org/10.1029/2007jd008632.
Zhang, X.Y., Wang, Y.Q., Niu, T., Zhang, X.C., Gong, S.L., Zhang, Y.M., Sun, J.Y., 2012. Atmospheric aerosol compositions in China: spatial/temporal variability, chemical signature, regional haze distribution and comparisons with global aerosols (vol. 12, pg 779, 2012). Atmos. Chem. Phys. 12, 6273. http://dx.doi.org/10.5194/acp-12-6273-2012.